

# Transport Limitation of Chlorine Disinfection of *Pseudomonas aeruginosa* Entrapped in Alginate Beads

Xiaoming Xu, Philip S. Stewart,\* and Xiao Chen  
Center for Biofilm Engineering, Montana State University,  
Bozeman, Montana 59717

Received April 8, 1995/Accepted August 8, 1995

An artificial biofilm system consisting of *Pseudomonas aeruginosa* entrapped in alginate and agarose beads was used to demonstrate transport limitation of the rate of disinfection of entrapped bacteria by chlorine. Alginate gel beads with or without entrapped bacteria consumed chlorine. The specific rate of chlorine consumption increased with increasing cell loading in the gel beads and decreased with increasing bead radius. The value of an observable modulus comparing the rates of reaction and diffusion ranged from less than 0.1 to 8 depending on the bead radius and cell density. The observable modulus was largest for large (3-mm-diameter) beads with high cell loading ( $1.8 \times 10^9$  cfu/cm<sup>3</sup>) and smallest for small beads (0.5 mm diameter) with no cells added. A chlorine microelectrode was used to measure chlorine concentration profiles in agarose beads (3.0 mm diameter). Chlorine fully penetrated cell-free agarose beads rapidly; the concentration of chlorine at the bead center reached 50% of the bulk concentration within approximately 10 min after immersion in chlorine solution. When alginate and bacteria were incorporated into an agarose bead, pronounced chlorine concentration gradients persisted within the gel bead. Chlorine did gradually penetrate the bead, but at a greatly retarded rate; the time to reach 50% of the bulk concentration at the bead center was approximately 46 h. The overall rate of disinfection of entrapped bacteria was strongly dependent on cell density and bead radius. Small beads with low initial cell loading (0.5 mm diameter,  $1.1 \times 10^7$  cfu/cm<sup>3</sup>) experienced rapid killing; viable cells could not be detected ( $<1.6 \times 10^5$  cfu/cm<sup>3</sup>) after 15 min of treatment in 2.5 mg/L chlorine. In contrast, the number of viable cells in larger beads with a higher initial cell density (3.0 mm diameter,  $2.2 \times 10^9$  cfu/cm<sup>3</sup>) decreased only about 20% after 6 h of treatment in the same solution. Spatially nonuniform killing of bacteria within the beads was demonstrated by measuring the transient release of viable cells during dissolution of the beads. Bacteria were killed preferentially near the bead surface. Experimental results were consistent with transport limitation of the penetration of chlorine into the artificial biofilm arising from a reaction-diffusion interaction. The methods reported here provide tools for diagnosing the mechanism of biofilm resistance to reactive antimicrobial agents in such applications as the treatment of drinking and cooling waters. © 1996 John Wiley & Sons, Inc.

Key words: disinfection • chlorine • transport • gel bead • biofilm • reaction-diffusion • *Pseudomonas aeruginosa*

## INTRODUCTION

Antimicrobial agents are widely applied in industrial and medical systems to control detrimental formation of microbial biofilms.<sup>21</sup> Unfortunately, bacteria growing as multicellular aggregates are invariably more resistant to antimicrobial treatments than are their freely suspended counterparts.<sup>4,6,13</sup>

The physical and biological mechanisms that render biofilm microorganisms less susceptible to biocides and antibiotics have yet to be established. One hypothesis to explain reduced susceptibility is that the bacteria and their exopolysaccharide products significantly reduce the penetration of antimicrobial agents.<sup>17</sup> Besides acting as a potential physical barrier to convective and diffusive transport, the microorganisms, exopolysaccharides, and other reactive constituents near the surface of the microbial aggregate could consume the antimicrobial agent, either by adsorption or by reaction, in large enough quantities to protect bacteria more deeply embedded. This hypothesis has been supported by experimental observations of biofilm disinfection.<sup>5,9,17</sup> Recently, a theoretical framework for the analysis of the reaction-diffusion interaction has been developed to explain these phenomena.<sup>22,23</sup> These efforts have touched upon fundamental mechanisms, but considerably more experimental work is required to verify this hypothesis and translate results to the application of antimicrobial agents in practice.

The purpose of the work reported in this article was to investigate experimentally the plausibility of transport limitation, arising from a reaction-diffusion interaction, as an explanation for the relative resistance of biofilms to reactive antimicrobial agents. To this end, we have used chlorine, a benchmark biocide, and artificial biofilms consisting of bacteria entrapped in alginate and agarose gel beads. Gel-immobilized bacteria are attractive as systems to study antimicrobial action against biofilms.<sup>12,25</sup> These systems mimic the basic structure of a biofilm—microorganisms dispersed in a hydrophilic polymer matrix—while providing the experimenter with reproducible control over the composition and geometry of the system. These latter features amount to a significant experimental advantage over natural biofilms, which are increasingly understood to be characterized by structural heterogeneity.<sup>7,16</sup>

\* To whom all correspondence should be addressed.

## THEORY

### Intraparticle Diffusion and Reaction

The relative rates of reaction and diffusion within the gel beads were evaluated by calculating a dimensionless observable modulus,  $\Phi$ , where

$$\Phi = \frac{R_o}{D_{\text{eff}}S_o} \left( \frac{V_p}{A_p} \right)^2 \quad (1)$$

and  $R_o$  is the overall chlorine removal rate (mg  $\text{Cl}_2$  removed/L s) which is proportional to the cell loading density,  $X$  (cfu/cm<sup>3</sup>),  $D_{\text{eff}}$  is the effective chlorine diffusivity in the beads (cm<sup>2</sup>/s),  $S_o$  is the bulk chlorine concentration (mg/L), and  $V_p$  and  $A_p$  denote the bead volume and external surface area, respectively. The diffusion coefficient in water was taken as  $1.44 \times 10^{-5}$  cm<sup>2</sup>/s.<sup>18</sup> An effective diffusivity of 90% of this value was used to account for the reduction in diffusion coefficient due to the presence of polymer.<sup>24</sup> The cell volume fraction in the gel beads was always less than 0.3%; the pore volume occupied by cells was therefore negligible in terms of its effect on diffusion. The utility of the modulus  $\Phi$  is that it can be calculated without knowledge of the reaction order or intrinsic kinetic parameters. It is based, rather, on the observed overall rate of reaction. When  $\Phi$  is sufficiently large ( $\Phi \geq 3$ ), the system can be diagnosed as transport limited. In contrast, when  $\Phi$  is small ( $\Phi \leq 0.3$ ), chemical reaction is the rate-limiting process.<sup>2</sup> This interpretation of  $\Phi$  assumes that external mass transfer resistance is negligible.

### External Film Mass Transfer Resistance

The external mass transfer coefficient  $k_L$  was estimated using correlations relating the Sherwood number ( $N_{\text{Sh}} = 2k_L r_p / D_{\text{aq}}$ ) to the Reynolds number ( $N_{\text{Re}} = 2U r_p / \nu_L$ ) and the Schmidt number ( $N_{\text{Sc}} = \nu_L / D_{\text{aq}}$ ). Here  $r_p$  is the bead radius (cm),  $D_{\text{aq}}$  is the chlorine diffusion coefficient in water (cm<sup>2</sup>/s),  $\nu_L$  is the solution kinematic viscosity (cm<sup>2</sup>/s), and  $U$  is the liquid velocity relative to the bead (cm/s). Here,  $U$  was assumed to be three times the terminal velocity in these calculations.<sup>14</sup> For  $N_{\text{Re}} < 30$ , the correlation derived by Brian and Hales<sup>3</sup> was used:

$$N_{\text{Sh}} = (4.0 + 1.21(N_{\text{Re}}N_{\text{Sc}})^{2/3})^{1/2} \quad (2)$$

For  $N_{\text{Re}} > 30$ , the relationship of Ranz and Marshall<sup>19</sup> was applied:

$$N_{\text{Sh}} = 2 + 0.6(N_{\text{Re}})^{1/2}(N_{\text{Sc}})^{1/3} \quad (3)$$

The effect of external mass transfer resistance on the overall rate of chlorine uptake was evaluated by examining the ratio of the observable modulus  $\Phi$  and a Biot number ( $N_{\text{Bi}}$ ) defined by

$$N_{\text{Bi}} = \frac{k_L r_p}{D_{\text{eff}}} \quad (4)$$

When  $\Phi/N_{\text{Bi}}$  is much smaller than unity, the influence of external film resistance is negligible.<sup>2</sup>

## MATERIALS AND METHODS

### Microorganisms

An environmental isolate of *Pseudomonas aeruginosa* (ERC1) was grown on Muller-Hinton agar plates (Difco, Detroit, MI) for 24 h. Colonies were harvested and washed by suspending in phosphate buffer (pH 7.2). The suspension was concentrated by centrifugation (10,000 rpm, 4°C, 10 min). Cell pellets were resuspended and diluted with phosphate buffer to desired concentrations.

### Immobilization Procedure

Five grams of bacterial suspension ( $3 \times 10^7$ – $6 \times 10^9$  cfu/mL) were mixed with 5 g of 4.0% (w/w) sodium alginate solution (Sigma Chemical Co.) to give a final gel concentration of 2% (w/w). This mixture was set in an ultrasonic water bath for 10 min to homogenize the mixture and eliminate air bubbles.

The cell-alginate mixture then was dropped through a hypodermic syringe into 50 mM  $\text{CaCl}_2$  solution to form beads. The size of the droplets was controlled by a coaxial air stream according to the method of Smidsrød.<sup>20</sup> Beads were gently stirred for 25 min in the gelling solution, then washed with 5 mM  $\text{CaCl}_2$  solution. Beads without cells were prepared in the same way but using phosphate buffer (pH 7.2) in place of the bacterial inoculum.

Agarose beads were prepared by dropping 2% agarose (Sigma) solution at 40°C into chilled water (4–6°C) with gentle magnetic stirring. To prepare agarose beads that also contained alginate, 4% agarose solution at 50°C was mixed with the same volume of 4% alginate solution with or without cells. The gel mixture, which contained 2% of each polymer, was then dropped into chilled water as described for the pure agarose beads. All immobilization procedures were carried out under aseptic conditions.

### Bead Size and Settling Velocity

Average bead diameter was measured by lining up 10 beads along the edge of a plastic ruler under a dissecting microscope. Terminal velocity of the gel beads in solution containing phosphate buffer and 5 mM  $\text{CaCl}_2$  was determined by measuring a bead's settling velocity in a 5-cm-diameter cylinder. Experiments were repeated three times under the same conditions.

### Disinfection and Chlorine Removal

Chlorine solutions (2.5–20 mg  $\text{Cl}_2$ /L) were prepared by diluting commercial bleach (Clorox) with phosphate buffer containing 5 mM  $\text{CaCl}_2$ . Chlorine concentration was deter-

mined by the *N,N*, diethyl-*p*-phenylenediamine (DPD) colorimetric standard method.<sup>1</sup> Disinfection, chlorine removal, and microelectrode experiments were conducted at  $26 \pm 1^\circ\text{C}$ .

In the disinfection experiments, approximately 0.5–1 g of beads containing cells were suspended in 1 L of 2.5 mg/L chlorine solution. A 3-cm-long magnetic stir bar was used to stir the flask. Five to 10 beads were sampled at various times and chlorine was immediately neutralized by placing the beads in a solution containing 100 mg/L sodium thiosulfate and 5 mM  $\text{CaCl}_2$ . To maintain a constant chlorine concentration, the solution in the flask was replaced about every 30 min. The maximum decrease of the chlorine concentration was about 0.2 mg/L in the 30-min period.

Measurements of chlorine consumption by reaction with gel beads were conducted in 250-mL stirred beakers. One gram of each kind of bead was suspended in 100 mL of chlorine solution in individual beakers. A beaker without added beads was used as a control. A 5-mL solution sample was taken from each beaker at various times to determine the chlorine concentration by the DPD colorimetric method.

Chlorine concentration data versus time were fit with fourth-order polynomials using the commercial software Sigmaplot (Jandel Scientific, San Rafael, CA). Overall chlorine removal rates,  $R_o$ , were determined from the derivative of the polynomials at various times. The observable modulus was then evaluated using Equation (1).

### Cell Enumeration

Beads were dissolved in 5 mL of 50 mM sodium citrate solution at  $4^\circ\text{C}$  for 12 h. Overall viable cell numbers in the beads were determined by colony formation on R2A agar.<sup>1</sup>

The spatial distribution of viable cells within the beads was determined by using a novel time-dependent dissolution technique. Ten gel beads were put into 10 mL of 50 mM sodium citrate solution. The tubes were vortex mixed (Thermolyne, type 37600) with 100% power input. It was experimentally demonstrated that the decrease of the bead radius was linearly related to the dissolution time. It took about 10 min to completely dissolve a 3-mm-diameter bead. A 0.1-mL portion of the supernatant was sampled at various times during dissolution for bacterial enumeration by plating on R2A agar. The bacterial density in different layers of the gel beads was calculated.

### Microelectrode Measurement of Chlorine Concentration Profiles

Microelectrode measurements were carried out in a simple batch reactor, as shown in Figure 1. A stainless steel screen and loop were used to hold the bead in a stirred chlorine solution. Agarose beads were used for the microelectrode experiments. The agarose beads contained alginic acid, but the alginate was not crosslinked with calcium. Calcium alginate gel beads were not suitable for probing with the microelectrode because the beads exhibited a tough outer surface layer that caused the bead to deform when probed.

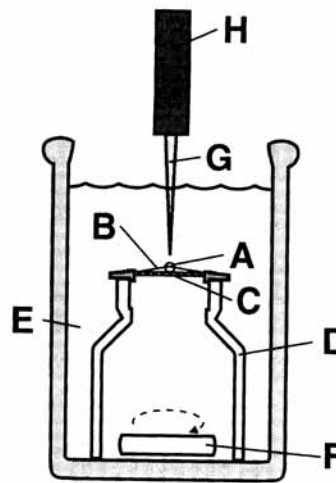


**Figure 1.** Apparatus for measurement of chlorine concentration profiles in gel beads. The bead A is held by stainless steel loop B and screen C. Screen C is supported by a plastic tube D which has openings near the bottom to allow circulation of the solution. The bead and holder are submerged in 20 mg/L chlorine solution E which is magnetically stirred by stir bar F. The microelectrode G is positioned using a computer-controlled step motor coupled to micromanipulator H.

Such distortion of alginate bead shape during microelectrode probing could give rise to artifacts, as others have indicated.<sup>15</sup> Agarose beads, on the other hand, were readily pierced by the microelectrode with no sign of deformation.<sup>10</sup>

An amperometric chlorine-sensitive microelectrode was prepared as described elsewhere.<sup>9</sup> The electrode consisted of a glass-covered platinum wire whose tip was exposed by grinding, etched to create a recession, and coated with a cellulose acetate film. A +0.2-V potential was applied relative to a saturated calomel electrode. Current was measured with a picoammeter (Keithley Instruments). To eliminate vibration of the electrode due to stirring, a short electrode with a sharply tapered tip (30  $\mu\text{m}$  diameter at the tip and about 75  $\mu\text{m}$  diameter 1 mm from the tip) was used. The probe was positioned using a computer-controlled step motor coupled to a micromanipulator. Step size was adjusted to 25  $\mu\text{m}$ . Immediately prior to each experiment, the electrode was calibrated using a chlorine solution assayed by the DPD colorimetric standard method. The microelectrode was positioned at the top center of the bead by a horizontal binocular microscope with 7–15 $\times$  magnification.

## RESULTS

### Intraparticle Reaction–Diffusion Limitation

Alginate beads with or without entrapped bacteria consumed chlorine. The observed rate of decrease of bulk chlorine concentration versus time in batch reactors varied with the bead radius and the cell density (Fig. 2). Beads with a higher cell loading and/or a larger surface area to volume

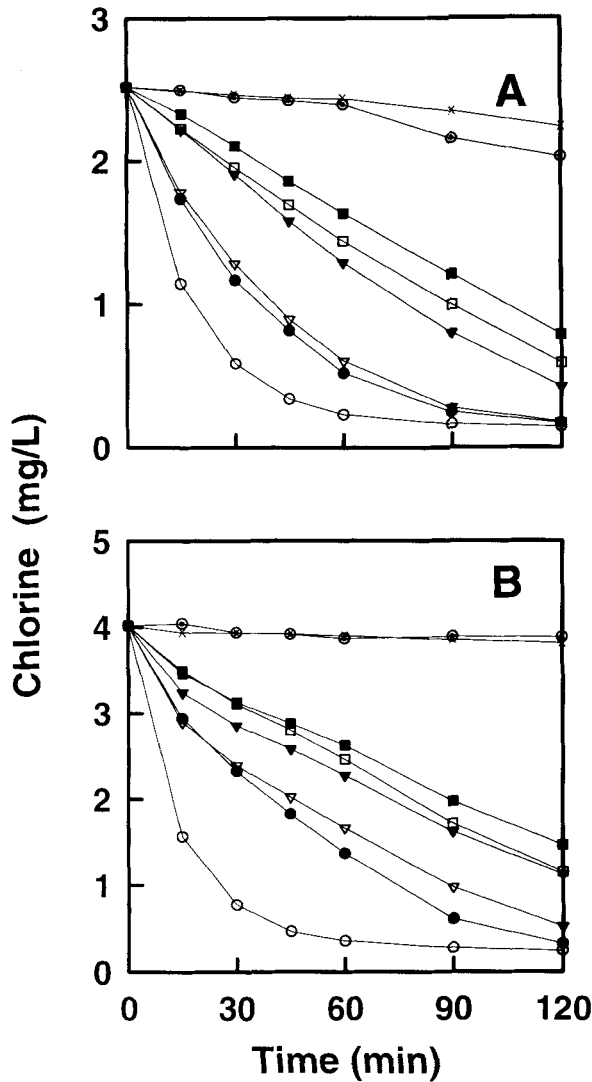


**Figure 2.** Consumption of chlorine by reaction with gel beads of various radii and cell loadings: (A) initial chlorine concentration 2.5 mg/L; (B) initial chlorine concentration 4 mg/L. Filled symbols indicate 3.0-mm-diameter beads and open symbols indicate 0.5-mm-diameter beads. The beads have the following diameters and cell loadings: (■) 3.0 mm, no cells; (▼) 3.0 mm,  $1.8 \times 10^8$  cfu/cm<sup>3</sup>; (●) 3.0 mm,  $1.8 \times 10^9$  cfu/cm<sup>3</sup>; (□) 0.5 mm, no cells; (▽) 0.5 mm,  $1.8 \times 10^8$  cfu/cm<sup>3</sup>; (○) 0.5 mm,  $1.8 \times 10^9$  cfu/cm<sup>3</sup>; (⊙) control 1, 3.0-mm agarose beads; (×) control 2, no beads.

ratio ( $A_p/V_p$ ) consumed more chlorine during the experimental period. For example, the initial chlorine removal rate for the small beads (0.5 mm diameter) with a cell density of  $1.8 \times 10^9$  cfu/cm<sup>3</sup> was 4.7 times higher than it was for beads with the same diameter but without cells. For gel beads with the same cell density, chlorine consumption by the small beads (0.5 mm diameter,  $A_p/V_p = 120$  cm<sup>-1</sup>) was about two times faster than for large beads (3.0 mm diameter,  $A_p/V_p = 20$  cm<sup>-1</sup>).

An observable modulus comparing the rates of reaction and diffusion was calculated using the experimental data shown in Figure 2. The modulus ranged from less than 0.1 to approximately 8 depending on the bead radius and cell

density (Fig. 3). All of the large beads (3.0 mm diameter) had observable modulus values higher than unity. Conversely, the modulus was smaller than unity for all experiments with small beads (0.5 mm diameter). The observable modulus was also cell-loading dependent since the beads with the highest cell loading ( $1.8 \times 10^9$  cfu/cm<sup>3</sup>) had the highest values of modulus for both size groups. The modulus was independent of chlorine concentration when the chlorine concentration was higher than 0.75 mg/L, but it decreased sharply when the chlorine concentration was lower than 0.75 mg/L.

### External Mass Transfer

External mass transfer coefficients ( $k_L$ ) were estimated using correlations taken from the literature along with exper-

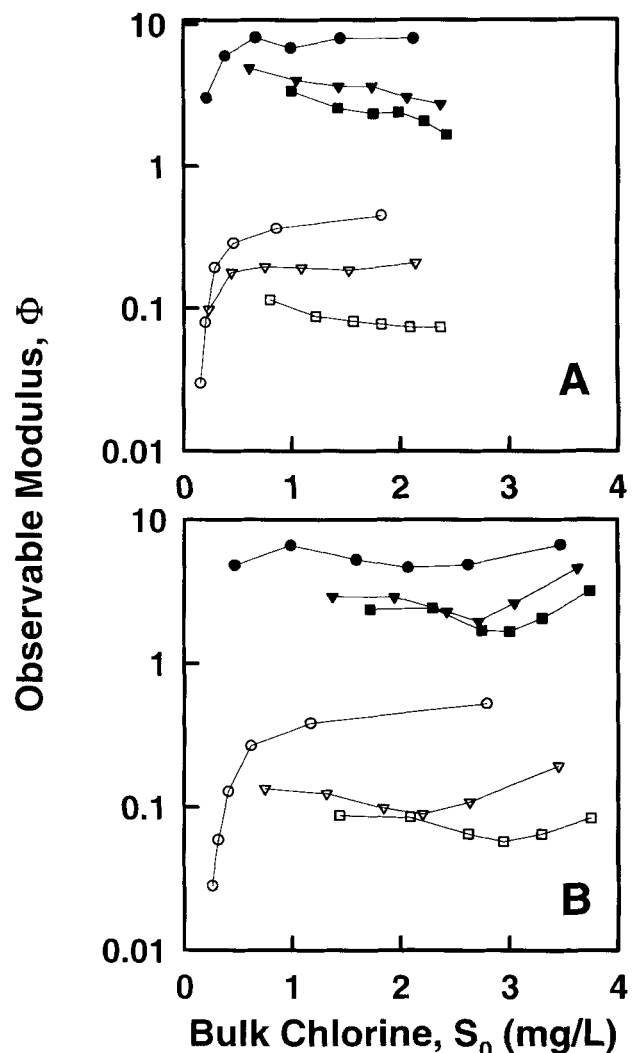


**Figure 3.** Observable modulus,  $\Phi$ , for reaction of chlorine with gel beads of various bead radii and cell loadings: (A) initial chlorine concentration 2.5 mg/L; (B) initial chlorine concentration 4 mg/L. The beads have the following diameters and cell loadings: (■) 3.0 mm, no cells; (▼) 3.0 mm,  $1.8 \times 10^8$  cfu/cm<sup>3</sup>; (●) 3.0 mm,  $1.8 \times 10^9$  cfu/cm<sup>3</sup>; (□) 0.5 mm, no cells; (▽) 0.5 mm,  $1.8 \times 10^8$  cfu/cm<sup>3</sup>; (○) 0.5 mm,  $1.8 \times 10^9$  cfu/cm<sup>3</sup>.

imentally determined bead terminal velocities. The terminal velocity was independent of cell loading. Terminal velocities for beads of various diameters are listed in Table I. The terminal velocity increased as the bead radius increased, but the calculated external mass transfer coefficient decreased. The ratio of the observable modulus and the Biot number ( $\Phi/N_{Bi}$ ) was much less than unity in all cases (Table I).

### Chlorine Penetration

Typical microelectrode-measured chlorine concentration profiles inside and outside of gel beads are shown in Figure 4. Significant external mass transfer resistance was not apparent as the chlorine concentration did not change by more than approximately 10% outside the bead. Chlorine penetrated cell-free agarose beads very fast; the chlorine concentration at the bead center reached 50% of its bulk concentration after only 10 min.

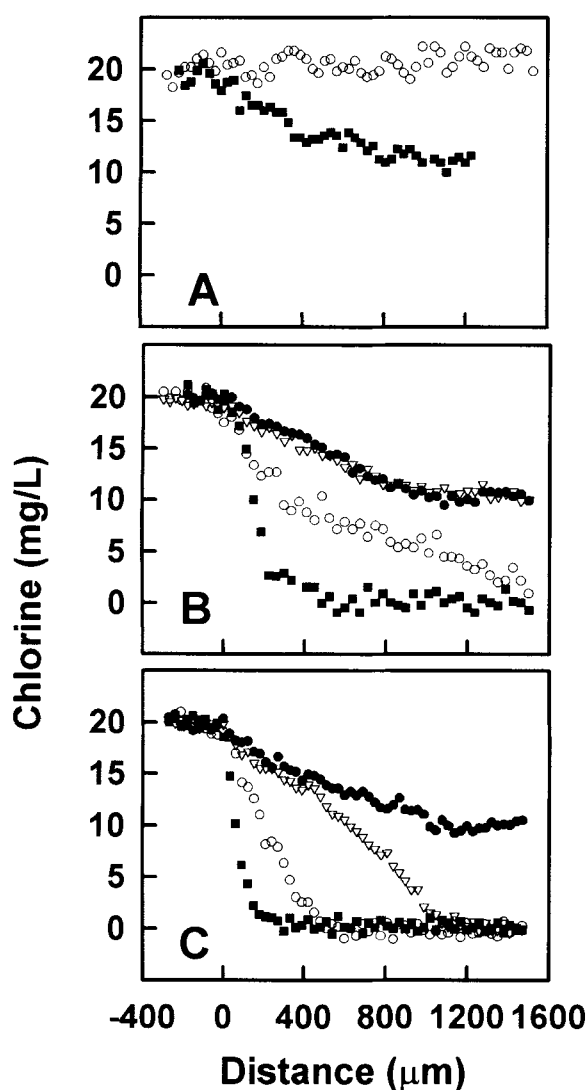


**Figure 4.** Microelectrode measurement of chlorine penetration into gel beads: (A) 2% agarose beads; (B) 2% agarose beads containing 2% alginate; (C) 2% agarose beads containing 2% alginate and  $2.5 \times 10^9$  cfu/cm<sup>3</sup> cells. Exposure time: (■) 10 min; (○) 2.5 h; (▽) 18 h; (●) 44 h.

centration after only 10 min. This was close to the theoretical value of 5 min for transient diffusion in a sphere without reaction.<sup>8</sup> After 2.5 h, the chlorine at the bead center was identical to its bulk concentration. However, for the agarose beads with 2% (w/w) alginate, the chlorine concentration at the bead center did not exceed 50% of its bulk concentration even after 45 h exposure. Penetration was even slower for agarose beads with 2% (w/w) alginate containing  $2.5 \times 10^9$  cfu/cm<sup>3</sup> cells.

### Overall Disinfection

When gel beads containing entrapped bacteria were treated with chlorine, the viable cell densities in the beads decreased with time (Fig. 5). The rate of disinfection depended on both the cell loading and the bead size. Medium-sized beads (1.2 mm diameter) with low initial cell loadings of about  $1.9 \times 10^8$  cfu/cm<sup>3</sup> experienced rapid killing; viable cell numbers decreased about two orders of magnitude after 30 min exposure. In contrast, viable cells in beads of the same diameter but with a higher initial cell loading ( $3.8 \times 10^9$  cfu/cm<sup>3</sup>) only decreased 30% during the same period. After 6 h exposure to 2.5 mg/L chlorine, the overall viable cell density in the large beads (2.8 mm diameter) with a high initial cell density  $2.2 \times 10^9$  cfu/cm<sup>3</sup> only experienced a 20% decrease, but viable cells could not be detected ( $<4 \times 10^3$  cfu/cm<sup>3</sup>) in the beads with lower initial cell density ( $1.6 \times 10^8$  cfu/cm<sup>3</sup>).

First-order disinfection rate coefficients ( $k_{dis}$ ) were calculated by linear regression of data shown in Figure 5 and from duplicate experiments. Observed disinfection rate coefficients should decrease monotonically as the observable modulus increases. To test this concept, the calculated disinfection rate coefficients were plotted as a function of  $r_p^2 X$  (Fig. 6). This dependence on bead radius and cell density is that embodied in the formulation of the observable modulus [Eq. (1)] if one recognizes that  $R_o$  is directly proportional to  $X$  and  $r_p^2$  is proportional to  $(V_p/A_p)^2$ . It was not possible to calculate the entire modulus because an independent estimate of the intrinsic reaction rate was lacking. The observed disinfection rate coefficients decreased slightly more than two orders of magnitude as  $r_p^2 X$  increased by a similar factor. The fact that  $k_{dis}$  correlates relatively smoothly with  $r_p^2 X$  suggests that the observable modulus adequately captures the dependence of disinfection on bead size and cell density.

### Spatial Distribution of Viable Cells Within Beads

The nonuniform spatial loss of viability within the gel beads during disinfection was demonstrated (Fig. 7). For beads with low initial cell loading (about  $1.2 \times 10^8$  cfu/cm<sup>3</sup>), cells near the bead surface were completely killed after only 15 min exposure. However, the killing of cells in the bead center took about 6 h. In contrast, cells in beads with a higher initial cell loading ( $2.5 \times 10^9$  cfu/cm<sup>3</sup>) were much more difficult to kill. After 6 h of treatment, only incom-

**Table I.** Evaluation of external film mass transfer resistance.

Parameter	Bead diameter 0.48 mm	Bead diameter 1.2 mm	Bead diameter 3.0 mm
Terminal velocity (cm/s)	0.43 ± 0.02	1.60 ± 0.08	2.55 ± 0.14
Mass transfer coefficient, $k_L$ (cm/s)	$5.41 \times 10^{-3}$	$5.19 \times 10^{-3}$	$4.03 \times 10^{-3}$
Schmidt number, $N_{Sc}$	619	619	619
Reynolds number, $N_{Re}$	7.0	65.2	258
Sherwood number, $N_{Sh}$	18.0	43.3	84.1
Biot number, $N_{Bi}$	9.02	21.6	42.0
Observable modulus, $\Phi$	0.07 ~ 0.29	ND	2.2 ~ 6.9
$\Phi/N_{Bi}$	0.008 ~ 0.032	ND	0.05 ~ 0.17

Note: In this calculation water kinematic viscosity ( $\nu_L$ ) was  $8.91 \times 10^{-3}$  cm<sup>2</sup>/s and the diffusivity of chlorine in water ( $D_{aq}$ ) was  $1.44 \times 10^{-5}$  cm<sup>2</sup>/s.

ND: not determined.

plete killing of cells near the surface of the bead was achieved.

## DISCUSSION

Perhaps the most straightforward explanation to account for the widely observed resistance of microbial biofilms to antimicrobial agents is that the antimicrobial compound simply fails to completely penetrate the biofilm. There are three phenomena that must be considered in evaluating the penetration of a solute into a biofilm or microbial aggregate: diffusion, partitioning, and reaction. The dynamics of diffusion by itself are readily assessed. The time scale for equilibration of a solute into a microbial aggregate by transient diffusion in the absence of partitioning or reaction is approximately  $(V_p/A_p)^2/D_{eff}$  where the characteristic aggregate

length is taken as the volume to surface area ratio  $V_p/A_p$  and  $D_{eff}$  is the solute effective diffusion coefficient in the aggregate.

For small solutes, theory and experiment suggest that effective diffusion coefficients within biofilm or immobilized cell particles are within approximately 50–90% of the diffusion coefficient of the solute in water.<sup>24</sup> With characteristic biofilm thicknesses of approximately hundreds to thousands of micrometers, the time scale for penetration is then expected to be on the order of minutes or tens of minutes at most. For example, our microelectrode measurement of chlorine penetration into a cell-free agarose gel bead is consistent with relatively quick diffusion. Chlorine concentration at the center of a 3-mm-diameter gel bead rose to 50% of the bulk fluid concentration in about 10 min (Fig. 4A). This is much quicker than typical antimicrobial dose durations which last for hours or days. Therefore, diffusion alone does not appear to be slow enough to explain reduced biofilm susceptibility.

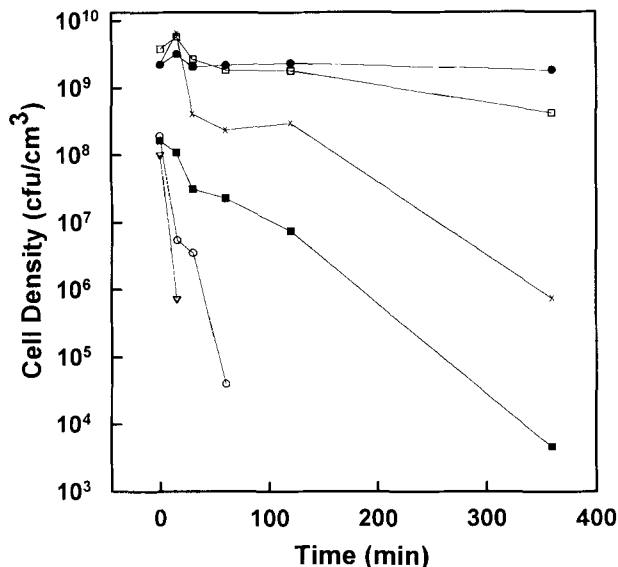


**Figure 5.** Overall disinfection of *P. aeruginosa* entrapped in gel beads of various bead radii and cell loadings. The bulk chlorine concentration was 2.5 mg/L. The beads have the following diameters and cell loadings: (■) 2.8 mm,  $1.6 \times 10^8$  cfu/cm<sup>3</sup>; (○) 1.2 mm,  $1.9 \times 10^8$  cfu/cm<sup>3</sup>; (▽) 0.4 mm,  $1.3 \times 10^8$  cfu/cm<sup>3</sup>; (●) 2.8 mm,  $2.2 \times 10^9$  cfu/cm<sup>3</sup>; (□) 1.2 mm,  $3.8 \times 10^9$  cfu/cm<sup>3</sup>; (×) 0.4 mm,  $2.3 \times 10^9$  cfu/cm<sup>3</sup>.

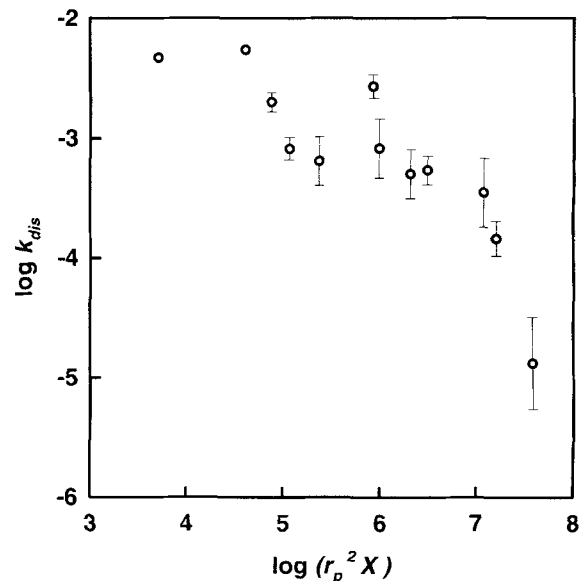


**Figure 6.** Dependence of overall disinfection rate coefficient,  $k_{dis}$  (s<sup>-1</sup>), on bead radius  $r_p$  (cm) and cell loading  $X$  (cfu/cm<sup>3</sup>).

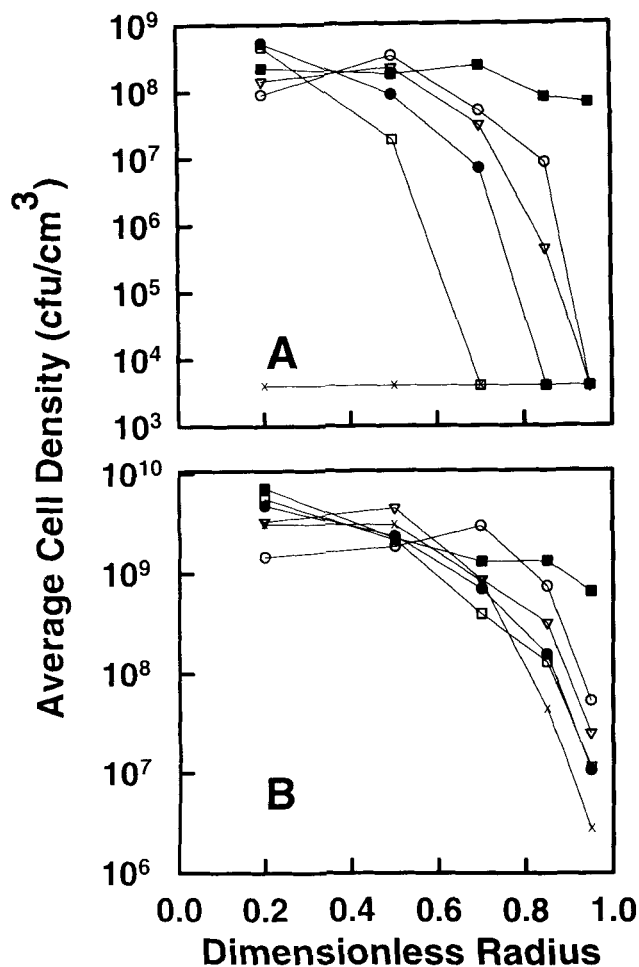


**Figure 7.** Spatial distribution of viable cells within gel beads during disinfection. Bead diameter is 3.0 mm. (A) Low initial cell loading ( $1.2 \times 10^8$  cfu/cm<sup>3</sup>). (B) High initial cell loading ( $2.5 \times 10^9$  cfu/cm<sup>3</sup>). Disinfection time: (■) 0 min; (○) 15 min; (▽) 30 min; (●) 60 min; (□) 120 min; (×) 360 min. Detection limit  $4 \times 10^3$  cfu/cm<sup>3</sup>.

If on the other hand the antimicrobial agent is consumed or otherwise neutralized in the microbial aggregate, then its penetration can be greatly retarded. An array of complementary experimental measurements in our artificial biofilm system support this hypothesis. Alginate gel beads with or without entrapped bacteria consumed chlorine, demonstrating that a neutralization reaction does occur (Fig. 2). Specific rates of chlorine consumption increased with increasing cell loading and decreased with increasing bead radius (Fig. 2). Such dependence on the physical structure of the microbial aggregate signals the impingement of transport limitation on the rate measurements. This interpretation is strengthened by calculation of an observable modulus comparing the rates of reaction and diffusion. The observable modulus was shown to exceed 1 in a number of cases indicating limitation by the rate of diffusive transport.

Direct measurement of chlorine penetration into agarose beads also supports a reaction-diffusion interaction. While chlorine fully penetrated cell-free agarose beads rapidly, beads incorporating alginate and bacteria exhibited pro-

nounced chlorine concentration gradients that persisted within the gel bead over a period of tens of hours (Fig. 4). These results agree with the measured reactivities of the various gel-cell systems. Pure agarose beads were the least reactive, while alginate beads containing bacteria were the most reactive (Fig. 1). The more reactive the gel bead, the slower the penetration of the biocide.

Measurements of the numbers of surviving bacteria in chlorine-treated gel beads are consistent with the above scenario. The overall rate of disinfection of entrapped bacteria was strongly dependent on the cell density and bead radius (Fig. 5). Small beads with low initial cell loading experienced rapid killing. In contrast, the number of viable cells in larger beads with a higher initial cell density decreased only about 20% after prolonged treatment in the same solution. Furthermore, it was shown by use of a novel technique that bacteria were killed preferentially near the bead surface (Fig. 7). The obvious explanation for survival of bacteria in the interior of the bead would appear to be that chlorine never penetrated to the bead center. Indeed, chlorine concentration profiles measured by a microelectrode (Fig. 4C) and viable cell concentrations (Fig. 7B) in similar bead systems approximately mirror each other. Near the bead surface chlorine concentrations are high and viable cell densities have been reduced. In the bead interior, chlorine concentrations approach zero and the viable cell density remains near its initial level. Viable cell profiles measured in this study are qualitatively similar to nonuniform patterns of respiratory activity measured within biofilms in response to monochloramine treatment.<sup>11</sup>

This work demonstrates that transport limitation can severely reduce the efficacy of a reactive antimicrobial agent (chlorine) against a biofilm. Experimental results are consistent with transport limitation of the penetration of chlorine into the artificial biofilm arising from a reaction-diffusion interaction. Reaction-diffusion theory, which is well developed in catalysis and immobilized cell engineering, can be adapted to explain these effects.<sup>23</sup> The results reported here support the application of this theory to engineer improvements to biofilm control programs.

Certain of the experimental methods we describe can be considered generic tools for diagnosing transport limitation of antimicrobial agents. In particular, gel beads provide a flexible, easily reproduced experimental system for evaluating the efficacy of antimicrobial agents against biofilms.<sup>25</sup> Gel beads can be thought of as artificial biofilms that can be tailored to simulate the microbiological, chemical, and physical characteristics representative of a particular application. The extent of transport limitation of the antimicrobial agent can be quantitatively assessed by performing simple batch measurements of the overall reaction rate of the antimicrobial agent with gel beads and then calculating an observable modulus. A novel technique for measuring the spatial profile of viable microorganisms within a gel bead can be used to determine the ability to disinfect organisms in different layers of the biofilm. Gel bead artificial biofilms permit quick, reproducible experiments and should prove

useful in the design of optimal strategies for controlling biofilm formation with antimicrobial agents.

This work was supported by the Center for Biofilm Engineering at Montana State University, a National Science Foundation supported Engineering Research Center (Cooperative agreement EEC-8907039), and by the Center's Industrial Associates. The software used to control the microelectrode was developed by Dong Chen.

## NOMENCLATURE

$A_p$	bead external surface area (cm <sup>2</sup> )
$D_{aq}$	chlorine diffusivity in water (cm <sup>2</sup> /s)
$D_{eff}$	effective chlorine diffusivity in bead (cm <sup>2</sup> /s)
$k_{dis}$	first-order disinfection rate (s <sup>-1</sup> )
$k_L$	external mass transfer coefficient (cm/s)
$N_{bi}$	Biot number (dimensionless)
$N_{Re}$	Reynolds number (dimensionless)
$N_{Sc}$	Schmidt number (dimensionless)
$N_{Sh}$	Sherwood number (dimensionless)
$r_p$	bead radius (cm)
$R_o$	overall chlorine removal rate in liquid (mg/L/s)
$S_o$	chlorine concentration in bulk liquid (mg/L)
$U$	liquid velocity (cm/s)
$V_p$	bead volume (cm <sup>3</sup> )
$X$	cell density in gel bead (cfu/cm <sup>3</sup> )

### Greek letters

$\nu_L$	solution kinematic viscosity (cm <sup>2</sup> /s)
$\Phi$	observable modulus

## References

- American Public Health Association, American Water Works Association, Water Environment Foundation. 1992. Standard methods for the examination of water and wastewater, 18th edition. American Public Health Association, Washington, DC.
- Bailey, J. E., Ollis, D. F. 1986. Biochemical engineering fundamentals, 2nd edition. McGraw-Hill, New York.
- Brian, P. L. T., Hales, H. B. 1969. Effects of transpiration and changing diameter on heat and mass transfer to spheres. *AIChE J.* **15**: 419-425.
- Characklis, W. G. 1990. Microbial biofouling control. pp. 585-634. In: W. G. Characklis and K. C. Marshall (eds.), *Biofilms*. J Wiley, New York.
- Chen, C.-I., Griebe, T., Characklis, W. G. 1993. Biocide action of monochloramine on biofilm systems of *Pseudomonas aeruginosa*. *Biofouling* **7**: 1-17.
- Costerton, J. W., Cheng K.-J., Geesey, G. G., Ladd, T. I., Nickel, J. C., Dasgupta, M., Marrie, T. J. 1987. Bacterial biofilms in nature and disease. *Ann. Rev. Microbiol.* **41**: 435-464.
- Costerton, J. W., Lewandowski, Z., de Beer, D., Caldwell, D., Korber, D., James, G. 1994. Biofilms, the customized microniche. *J. Bacteriol.* **176**: 2137-2142.
- Crank, J. 1975. The mathematics of diffusion, 2nd edition. Oxford Science Publications, Oxford.
- de Beer, D., Srinivasan, R., Stewart, P. S. 1994. Direct measurement of chlorine penetration into biofilms during disinfection. *Appl. Environ. Microbiol.* **60**: 4339-4344.
- Hooijmans, C. M., Ras, C., Luyben, K. Ch. A. M. 1990. Determination of oxygen profiles in biocatalyst particles by means of a combined polarographic oxygen microsensor. *Enz. Microb. Technol.* **12**: 178-183.
- Huang, C.-T., Yu, F. P., McFeters, G. A., Stewart, P. S. 1995. Non-uniform spatial patterns of respiratory activity within biofilm during disinfection. *Appl. Environ. Microbiol.* **61**: 2252-2256.
- Jouenne, T., Tresse, O., Junter, G.-A. 1994. Agar-entrapped bacteria as an in vitro model of biofilms and their susceptibility to antibiotics. *FEMS Microbiol. Lett.* **119**: 237-242.
- LeChevallier, M. W., Hassenauer, T. S., Camper, A. K., McFeters, G. A. 1984. Disinfection of bacteria attached to granular activated carbon. *Appl. Environ. Microbiol.* **48**: 918-923.
- Monbouquette, H. G., Sayles, G. D., Ollis, D. F. 1990. Immobilized cell biocatalyst activation and pseudo-steady-state behaviors: Model and experiment. *Biotechnol. Bioeng.* **35**: 609-629.
- Müller, W., Winnefeld, A., Kohls, O., Scheper, T., Zimelka, W., Baumgärtel, H. 1994. Real and pseudo oxygen gradients in Ca-alginate beads monitored during polarographic P<sub>o2</sub>-measurements using Pt-needle microelectrodes. *Biotechnol. Bioeng.* **44**: 617-625.
- Murga, R., Stewart, P. S., Daly, D. 1995. Quantitative analysis of biofilm thickness variability. *Biotechnol. Bioeng.* **44**: 503-510.
- Nichols, W. W., Evans, M. J., Slack, M. P. E., Walmsley, H. L. 1989. The penetration of antibiotics into aggregates of mucoid and non-mucoid *Pseudomonas aeruginosa*. *J. Gen. Microbiol.* **135**: 1291-1303.
- Perry, R. H., Chilton, C. H. 1973. Chemical engineer's handbook, 5th edition. McGraw-Hill, New York.
- Ranz, W. E., Marshall, W. R. 1952. Evaporation from drops. Part II. *Chem. Eng. Prog.* **48**: 173-180.
- Smidsrød, O., Skjåk-Bræk, G. 1990. Alginate as immobilization matrix for cells. *Trends Biotechnol.* **8**(3): 71-78.
- Srinivasan, R., Stewart, P. S., Griebe, T., Chen, C.-I., Xu, X. 1995. Biofilm parameters influencing biocide efficacy. *Biotechnol. Bioeng.* **46**: 553-560.
- Stewart, P. S. 1994. Biofilm accumulation model that predicts antibiotic resistance of *Pseudomonas aeruginosa* biofilms. *J. Antimicrob. Chemother.* **38**: 1052-1058.
- Stewart, P. S., Raquepas, J. B. 1995. Implications of reaction-diffusion theory for the disinfection of microbial biofilms by reactive antimicrobial agents. *Chem. Eng. Sci. (to appear)*.
- Westrin, B. A., Axelsson, A. 1991. Diffusion in gels containing immobilized cells: A critical review. *Biotechnol. Bioeng.* **38**: 439-446.
- Whitham, T. S., Gilbert, P. D. 1993. Evaluation of a model biofilm for the ranking of biocide performance against sulphate-reducing bacteria. *J. Appl. Bacteriol.* **75**: 529-535.